Decay Parameters for $\Sigma^{\pm} \to n\pi^{\pm}$

ROGER O. BANGERTER, MARGARET ALSTON-GARNJOST, ANGELA BARBARO-GALTIERI, LAWRENCE K. GERSHWIN, TERRY S. MAST, JOSEPH J. MURRAY, FRANK T. SOLMITZ, M. LYNN STEVENSON, AND ROBERT D. TRIPP

Lawrence Radiation Laboratory, University of California, Berkeley, California 94720

(Received 1 August 1969)

In this paper, we present measurements of the decay parameters $\phi_{\pm}$ for $\Sigma^{\pm} \to n\pi^{\pm}$. The usual decay parameters α, β, and γ are related to ϕ by the equation $\beta = (1-\alpha^2)^{\frac{1}{2}}\sin\phi$ and $\gamma = (1-\alpha^2)^{\frac{1}{2}}\cos\phi$. Polarized $\Sigma^{\pm}$ were produced by the reactions $K^- p \to \Sigma^{\pm}\pi^{\mp}$ in the Lawrence Radiation Laboratory's 25-in. hydrogen bubble chamber. The average momentum of the incident K^- beam was 385 MeV/c. The measurements of $\phi_{\pm}$ were made by observing the left-right asymmetry in the np interactions of those decay neutrons that subsequently scattered on the hydrogen in the bubble chamber. We obtain $\phi_- = 14 \pm 19$ deg and $\phi_+ = 143 \pm 29$ deg. Since $\gamma = (|s|^2 - |p|^2)/(|s|^2 + |p|^2)$, this shows that $\Sigma^- \to n\pi^-$ takes place predominantly in the s wave, whereas $\Sigma^+ \to n\pi^+$ is dominated by p-wave decay. These results are in agreement with the $\Delta I = \frac{1}{2}$ rule.

I. INTRODUCTION

THE $K^- p$ interaction at 390 MeV/c is a copious source of well-polarized Σ hyperons. This experiment, which was performed at the Bevatron with the LRL 25-in. hydrogen bubble chamber, makes use of this fact to obtain a large sample of nonleptonic Σ decays suitable for the determination of $\phi_{\pm}$.

The nonleptonic Σ decays $\Sigma^{\pm} \to n\pi^{\pm}$ and $\Sigma^+ \to p\pi^0$ are conventionally parametrized in terms of their decay rates and the three parameters α, β, and γ, defined as

$$\alpha = \frac{2\,\mathrm{Re}(s^* p)}{|s|^2 + |p|^2}, \quad \beta = \frac{2\,\mathrm{Im}(s^* p)}{|s|^2 + |p|^2}, \quad \gamma = \frac{|s|^2 - |p|^2}{|s|^2 + |p|^2},$$

where s and p are, respectively, the s- and p-wave decay amplitudes. Since $\alpha^2 + \beta^2 + \gamma^2 = 1$ it is convenient to introduce an additional parameter ϕ defined by

$$\beta = (1-\alpha^2)^{1/2}\sin\phi, \quad \gamma = (1-\alpha^2)^{1/2}\cos\phi.$$

Also the likelihood function for ϕ is more nearly Gaussian than that for β or γ. A subscript $+$, $-$, or 0 on any of these parameters indicates the charge of the decay pion.

Our definitions of parameters, sign conventions, and notation are the same as those of the Particle Data Group.[1] In particular, for unpolarized Σ hyperons, α is equal to the helicity of the decay nucleon.

Earlier experiments[2,3] indicate that α_+ and α_- are nearly equal to zero, while α_0 is nearly equal to -1. If time-reversal invariance holds, the phases of s and p are given by the πN scattering phase shifts evaluated at the decay energy. Since these phase shifts are small, β_+ and β_- are also expected to be small.

If α and β are equal to zero, then $\gamma = \pm 1$, and the decay proceeds entirely through the s- or the p-wave channel. In addition, the $\Delta I = \frac{1}{2}$ rule requires that if $\gamma_+ = \pm 1$, then $\gamma_- = \mp 1$.[2] There are theoretical predictions that $\gamma_+ = -1$.[4] Our results are in agreement with these predictions, and are also in agreement with the measurements by Berley *et al.*[3]

The polarization of the neutron in $\Sigma^{\pm} \to n\pi^{\pm}$ is given by

$$\mathbf{P}_n = [(\alpha + \mathbf{P}_\Sigma \cdot \mathbf{q})\mathbf{q} + \beta(\mathbf{P}_\Sigma \times \mathbf{q}) + \gamma\mathbf{q} \times (\mathbf{P}_\Sigma \times \mathbf{q})]/(1 + \alpha\mathbf{P}_\Sigma \cdot \mathbf{q}), \quad (1)$$

where $\mathbf{q}$ is a unit vector along the momentum of the neutron and $\mathbf{P}_\Sigma$ is the polarization of the Σ.

Apart from measured kinematical quantities, $\mathbf{P}_n$ is dependent on α, $\mathbf{P}_\Sigma$, and ϕ. Both α and $\mathbf{P}_\Sigma$ can be determined independently of (1), so that $\mathbf{P}_n$ becomes a function of the single unknown parameter ϕ. The polarization $\mathbf{P}_n$, and hence ϕ, is measured by observing the left-right asymmetry in the np interactions of those decay neutrons that subsequently scatter on the hydrogen in the bubble chamber. Figure 1 illustrates the complete sequence of reactions for a Σ^- event.

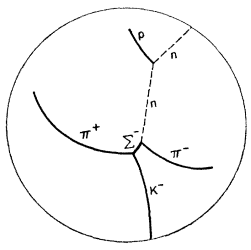

FIG. 1. Typical Σ^- event with np scattering.

[1] Particle Data Group, Rev. Mod. Phys. **41**, 109 (1969).

[2] R. O. Bangerter, A. Barbaro-Galtieri, J. P. Berge, J. J. Murray, F. T. Solmitz, M. L. Stevenson, and R. D. Tripp, Phys. Rev. Letters **17**, 495 (1966).

[3] D. Berley, S. Hertzbach, R. Kofler, S. Yamamoto, W. Heintzelman, M. Schiff, J. Thompson, and W. Willis, Phys. Rev. Letters **17**, 1071 (1966); D. Berley, S. Hertzbach, R. Kofler, G. Meisner, J. B. Shafer, S. Yamamoto, W. Heintzelman, M. Schiff, J. Thompson, and W. Willis, *ibid.* **19**, 979 (1967). The 1966 results of Berley *et al.* were the first conclusive evidence that $\Sigma^+ \to n\pi^+$ is dominated by p-wave decay. Their results on $\Sigma^- \to n\pi^-$ as well as our preliminary results for $\Sigma^{\pm} \to n\pi^{\pm}$ [University of California Radiation Laboratory Report No. UCRL-17781 (unpublished)] were presented to the *Heidelberg International Conference on Elementary Particles, Heidelberg, 1967*, edited by H. Filthuth (North-Holland Publishing Company, Amsterdam, 1968). Suggestive evidence in agreement with these results was obtained in 1965 by analyzing $\Sigma^{\pm} \to n\pi^{\pm}\gamma$. See M. Bazin, H. Blumenfeld, U. Nauenberg, and L. Seidlitz, Phys. Rev. **140**, B1358 (1965).

[4] H. Sugawara, Phys. Rev. Letters **15**, 870 (1965); **15**, 997 (1965); M. Suzuki, *ibid.* **15**, 986 (1965).

In Sec. II, we discuss the determination of P_Σ and, in Sec. III, the measurement of ϕ.

II. DETERMINATION OF P_Σ

Watson, Ferro-Luzzi, and Tripp[5] have shown that the Σ's produced by the K^-p interaction in the vicinity of the $Y_0^*(1520)$ are highly polarized owing to the interference of the resonant $D_{3/2}$ amplitude with the large s-wave background. This analysis, based on about 2300 Σ events, was corroborated by our later analysis of 15 000 Σ events.[2]

Since α_0 is nearly -1, the Σ^+ polarization is readily observable through the up-down asymmetry given by the familiar decay distribution

$$I=1+\alpha\mathbf{P}_\Sigma\cdot\mathbf{q}. \tag{2}$$

In contrast α_- is very small, so that it is impractical to measure well the Σ^- polarization through the up-down asymmetry. Consequently, one must rely on the values obtained from the production amplitudes. In order to determine these amplitudes more precisely, we have recently completed a preliminary multichannel partial-wave analysis with about 140 000 charged Σ events. The beam momentum ranged from 280 to 470 MeV/c, however, 90% of the events used for the measurement of ϕ have beam momenta between 360 and 420 MeV/c. The polarizations obtained from this analysis are shown in Figs. 2(a) and 2(b), and are in substantial agreement with the previous work. The sign convention is such that

$$\mathbf{P}_\Sigma=P_\Sigma(\mathbf{K}\times\boldsymbol{\pi})/|\mathbf{K}\times\boldsymbol{\pi}|, \tag{3}$$

where $\mathbf{K}$ and $\boldsymbol{\pi}$ are along the incident K^- and the production π. The points $-\alpha_0 P_{\Sigma^+}$ as measured from (2) are shown superimposed on the curves of Fig. 2(a). It is evident that α_0 is nearly equal to -1, that the fits are good, and that the Σ^+ polarization is well determined, particularly in the neighborhood of 385 MeV/c, where the vast majority of events lie.

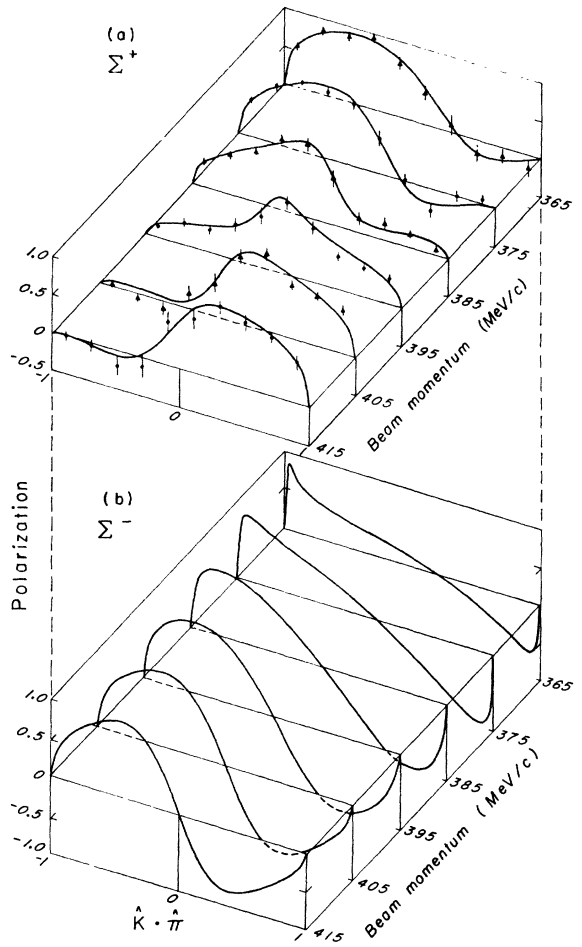

FIG. 2. Calculated values of Σ polarization as a function of beam momentum and production cosine. The data points are measured values of $-\alpha_0 P_{\Sigma^+}$.

We emphasize that, despite the lack of any dynamical theory of the strong interactions, the calculated Σ^- polarization (P_{calc}) should be quite reliable. The major assumptions are unitarity, isospin conservation, a Breit-Wigner form for the resonant amplitude, and smooth energy dependence for the nonresonant amplitudes. Furthermore the momentum is low, so only a few partial waves are significant. The resonant amplitude interferes with the nonresonant amplitudes in such a way as to produce spectacularly rapid variations in the angular distributions. This condition allows a precise determination of the parameters of the resonance.

We have fitted our data to two different models consistent with the above assumptions: (a) that used by Watson, Ferro-Luzzi, and Tripp, which parametrizes the nonresonant amplitudes in terms of constant scattering lengths, and (b) the K-matrix formalism of Ross and Shaw,[6] as used, for example, by Kim.[7] The two models give very similar results for P_{calc}. For our events the rms value of P_{calc} is equal to 0.6100 for model (a) and 0.6085 for model (b).

Although our partial-wave analysis is preliminary, we are confident that all major sources of bias have been detected and eliminated. In any event the uncertainties in the polarizations are almost certainly smaller than the statistical uncertainty in our measurement of ϕ.

If α_- is not truly zero, it is possible to confirm crudely the Σ^- polarizations. We have divided our sample of 60 000 Σ^- events into four bins according to P_{calc}. The first bin contains those events with $-1<P_{\text{calc}}<-0.5$, the second contains those with $-0.5<P_{\text{calc}}<0$, and so on. For each bin, $\alpha_- P_{\Sigma^-}$ was measured by fitting to Eq. (2). Figure 3 shows $\alpha_- P_{\Sigma^-}$ as a function P_{calc}. The points are plotted at the mean value of P_{calc} for each bin. If the predicted polarizations are correct, the points

[5] M. B. Watson, M. Ferro-Luzzi, and R. D. Tripp, Phys. Rev. **131**, 2248 (1963).

[6] M. Ross and G. Shaw, Ann. Phys. (N. Y.) **13**, 147 (1961).

[7] J. K. Kim, Phys. Rev. Letters **19**, 1074 (1967).

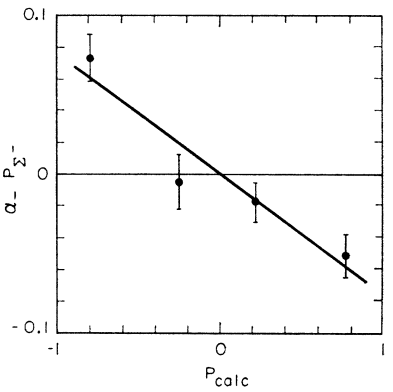

FIG. 3. Measured values of $\alpha_- P_{\Sigma^-}$ as a function of the calculated polarization P_{calc}.

should lie on a straight line with slope α. The line shown is the best least-squares fit to our data, and has a slope of -0.076. The data clearly exclude a slope of zero and do provide weak evidence confirming the shape, but not the sign, of the curves in Fig. 2(b).

III. MEASUREMENT OF ϕ

As explained above, we measure ϕ by observing the angular distribution of np scatterings produced by the reactions $\Sigma^{\pm} \to \pi^{\pm} n$; $np \to np$. The probability density for the np reaction is given by

$$W(\mathbf{P}_n \cdot \mathbf{s}) d\zeta = \tfrac{1}{2}(1 + A \mathbf{P}_n \cdot \mathbf{s}) d\zeta , \qquad (4)$$

where $\mathbf{s}$ is the unit normal to the np scattering plane and A is the np scattering asymmetry. The azimuthal scattering angle ζ is given by $\zeta = \cos^{-1}(\mathbf{P}_n \cdot \mathbf{s}/|\mathbf{P}_n|)$. We use the values of A determined by Arndt and MacGregor.[8]

The vector $\mathbf{P}_n$ appearing in (4) is the polarization of the neutron, as observed in that rest frame of the neutron obtained by a direct Lorentz transformation from the np center-of-mass system, while $\mathbf{P}_n$ as given by (1) is measured in that rest frame of the neutron obtained by a Lorentz transformation along $\mathbf{q}$ from that Σ rest frame (ΣRF) in which $\mathbf{q}$ and $\mathbf{P}_\Sigma$ are measured. The polarization $\mathbf{P}_\Sigma$ as given by (3) is correct in either the ΣRF obtained by a direct Lorentz transformation from the laboratory ($\Sigma\mathrm{RF}_{\mathrm{lab}}$) or the ΣRF obtained by a transformation from the $K^- p$ center-of-mass system.

Because of the curvature of the Σ in the magnetic field of the bubble chamber, $\Sigma\mathrm{RF}_{\mathrm{lab}}$ rotates. Furthermore both $\mathbf{P}_\Sigma$ and $\mathbf{P}_n$ precess. Owing to the short Σ mean life, these effects result in a negligible change in $\mathbf{P}_\Sigma$, but for a low-momentum neutron $\mathbf{P}_n$ can change by more than a radian.

For simplicity in writing equations we will continue to use the nonrelativistic notation. In particular, we make no distinction between $\mathbf{P}_n$ in (1) and $\mathbf{P}_n$ in (4). However, in performing all calculations we employ the following procedure.

The polarization $\mathbf{P}_n$ in (1) is generalized to a four-vector.[9] We transform this four-vector to $\Sigma\mathrm{RF}_{\mathrm{lab}}$ and from $\Sigma\mathrm{RF}_{\mathrm{lab}}$ to the laboratory frame. In the laboratory system, the precession of $\mathbf{P}_n$ is easily calculated owing to the simple form of the electromagnetic field strength tensor. The remaining transformation to the frame appropriate to (4) is unnecessary since $\mathbf{P}_n \cdot \mathbf{s}$ would be unchanged.

A. Identification of Events

The relatively low K^- yield of the Bevatron and rapid decay of a low-momentum K^- beam necessitated placing the bubble chamber very close to the Bevatron, thus precluding the use of adequate shielding against background. In particular, a high background flux of fast neutrons produced about 20 np scatterings per frame, making it impossible to select the real events simply by scanning.

In order to select those scatterings resulting from Σ decay, we first measured and analyzed about 20 000 events of the type $\Sigma^+ \to n\pi^+$ and 52 000 events of the type $\Sigma^- \to n\pi^-$. We rejected those events having a neutron momentum less than 275 MeV/c. At these low momenta, A is very small and the events would not significantly contribute to our results. Elimination of the low-momentum neutrons reduced the total sample to about 43 000 events. The results of the analysis of these 43 000 events were used to predict the direction of the neutrons on the scanning projector in three different views. We then scanned for np scatterings that occurred within ± 3 deg of the predicted direction in all three views.[10] The scanners were requested to record only those events in which the projected length of the proton track (on the scanning projector with a magnification of $\frac{2}{3}$) was at least 2 mm in one view and not less than 1 mm in any view. Both scanning efficiency and measuring accuracy are poor for very short-track protons; we therefore increased the above lengths to 4 and 2 mm, respectively, for those events actually used in the determination of ϕ.

The above selection procedure was very effective. From a total of $43\,000 \times 20 = 860\,000$ np scatterings only approximately 4300 events satisfying the scanning criteria were found. The recoil protons were measured and the results of these measurements were merged with the original measurements of Σ production and decay. The resulting data were subjected to a seven-constraint (7C) three-vertex fit. In some cases, which constitute 4% of the fitted events, the momentum of the recoil proton cannot be measured with sufficient

[8] Richard A. Arndt (private communication). However, the values used by us are very similar to those determined by the analysis by M. H. MacGregor, R. A. Arndt, and R. M. Wright, Phys. Rev. 182, 1714 (1969).

[9] V. Bargmann, L. Michel, and V. L. Telegdi, Phys. Rev. Letters 2, 435 (1959).

[10] In almost all cases the direction of the neutron can be predicted to better than 1 deg. In those cases in which it cannot, the 3-deg scanning criterion was extended to ± 3 standard deviations.

accuracy to provide any real constraint. These events were fitted with the use of only six constraints. We obtain a final sample of 1385 Σ^- events and 560 Σ^+ events.

B. Estimation of Background

The original fit to Σ production and decay is 4C,[11] and, as noted, this fit determines both the direction and momentum of the neutron. Two of the three additional constraints imposed by measuring the *np* scattering can be regarded as coming from the measurement of the position of the *np* interaction point. Since the position of the $\Sigma \rightarrow n\pi$ vertex is known, this is equivalent to measuring the two angles specifying the direction of the neutron.

The neutron momentum and measurement of the *np* scattering angle determine the proton momentum. Measurement of this momentum provides the third additional constraint.

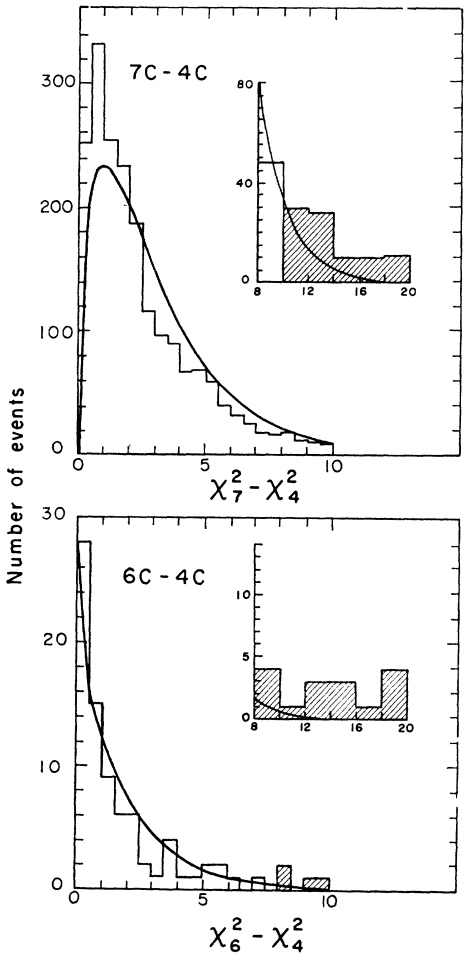

FIG. 4. Distributions of $\chi_7^2-\chi_4^2$ and $\chi_6^2-\chi_4^2$.

[11] The length of the Σ track is typically too short to permit a useful momentum measurement; otherwise the fit to Σ production and decay would be 5C.

We estimate that the accuracy with which the direction of the neutron is known is alone sufficient to reduce background contamination to 10%. In order to investigate the elimination of background effected by all three constraints, we subtracted χ_4^2—the χ^2 for the 4C fit—from χ^2 for the final 7C or 6C fit. It can be shown that this difference is distributed as χ_3^2 (or χ_2^2). The experimental χ^2 distributions together with the expected distributions are shown in Fig. 4. The experimental distributions are too narrow, indicating a slight overestimation of uncertainties. After examining these curves we decided to reject those events falling in the shaded areas of Fig. 4.

The χ^2 distribution for n degrees of freedom is given by

$$W_n(\chi^2)d\chi^2 \propto e^{-\chi^2/2}(\chi^2)^{n/2-1}d\chi^2. \quad (5)$$

If the background is random rather than Gaussian, the χ^2 distribution for background events by comparison with (5) is given by

$$W_n(\chi^2)d\chi^2 \propto (\chi^2)^{n/2-1}d\chi^2. \quad (6)$$

The background is not, of course, truly random, but has some probability density function of finite width. An analysis of the distributions of the background events, including the effects of the ± 3-deg scanning criterion, indicates that the deviations from (6) for $(\chi_7^2-\chi_4^2)<20$ or for $(\chi_6^2-\chi_4^2)<20$ are very small.

We obtain an upper limit on contamination of 2.9% by normalizing (6) to the shaded areas in Fig. 4, assuming that all events in these areas are background. This should be a considerable overestimation for two reasons: The number of true events falling in this region is predicted by (5) to be about 2% of the total. Allowing for the overestimation of errors one expects this to be reduced to 0.5–1%. In addition, the χ^2 distributions for bubble chamber experiments, in our experience, always have considerably more genuine events with large χ^2 than Eq. (5) predicts.

As final check on the effect of background, the unshaded areas in Fig. 4 were both extended to $\chi^2=16$. According to (6), this doubles the background in the sample, but results in a shift in ϕ_+ and ϕ_- of less than 8% of the statistical uncertainty. We conclude that the effects of background are truly negligible.

C. Investigation of Biases

In addition to contamination, the opposite problem of loss of real events could also produce a bias. One expects the three major sources of loss to be (a) bad measurements, (b) scanning inefficiency, and (c) loss of protons that leave the bubble chamber close to the point of interaction. The problem of bad measurements was considerably mitigated by carefully inspecting, and remeasuring, if necessary, all those events in which the recoil proton could not be successfully reconstructed from the original measurements. Altogether, 18% of the original 4300 events were remeasured.

Scanning efficiency and loss of particles that leave the bubble chamber shortly after scattering should both be primarily functions of the projected length of the recoil proton. In order to investigate these effects, 16% of our film was rescanned. Scanning efficiencies based on the two scans show a striking deficiency of short-track protons. However, since scanners on both scans tend to miss the same events and because of insufficient data, efficiencies based on this method are not reliable.

Since np cross sections and polarizations are well known, we decided to obtain detection efficiencies by comparing the outcome of the actual experiment with the results of a Monte Carlo simulation.

The neutron from each of the 43 000 original Σ decays was propagated through the bubble chamber 10 times, producing about 33 000 fake np scatterings distributed according to the known cross section. The differential cross section depends on $\mathbf{P}_n$, which in turn is a function of ϕ and $\mathbf{P}_\Sigma$. The Monte Carlo simulation was performed for several extreme combinations of ϕ and P_Σ. Fortunately all simulations give essentially the same detection efficiencies.

The detection efficiency e is given by

$$e=10\frac{\text{(true events)}}{\text{(Monte Carlo events)}}.$$

Note that this is an over-all detection efficiency and includes losses due to all effects. We find e to be a function of two parameters: The first, as expected, is the projected length of the proton. Since the scanners scanned in only one view unless an event was found, the projected length was taken to be the length in this view. Additionally, we find that those protons which dip steeply in the chamber are preferentially missed. This is presumably because the photographic perspective is such that these tracks appear considerably different in the three views and are not recognized by the scanners as the same event. The detection efficiency as a function of projected length for those protons with dip angles λ less than and greater than 45 deg is shown in Fig. 5. The curves are freehand and reflect the belief that the detection efficiency as a function of projected length should increase monotonically and then form a plateau.

D. Maximum-Likelihood Determination of ϕ

The probability density (4) must now be altered to include the effects of detection efficiency. We represent e as a function of ζ and a set of parameters y, describing all other relevant aspects of a particular event. Let $Q(y)$ be the probability density for y. Then (4) becomes

$$W(\phi,\zeta)d\zeta=\frac{[1+AP_n(\phi)\cos\zeta]\int e(\zeta,y)Q(y)dy}{\int[1+AP_n(\phi)\cos\zeta]e(\zeta,y)Q(y)d\zeta\,dy}d\zeta. \quad (7)$$

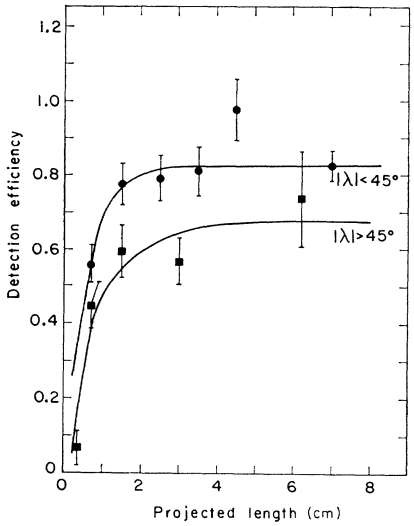

FIG. 5. Detection efficiency as a function of projected length for dip angles λ less than and greater than 45°.

We form the likelihood function $\mathfrak{L}(\phi)$, using Eq. (7). Neglecting terms independent of ϕ, $\ln\mathfrak{L}(\phi)$ is given by

$$\ln\mathfrak{L}(\phi)=\sum\ln[1+AP_n(\phi)\cos\zeta]-N\ln\int[1+AP_n(\phi)\cos\zeta]e(\zeta,y)Q(y)d\zeta\,dy.$$

The sum extends over the total number of events N. This sum is just the usual expression for $\ln\mathfrak{L}(\phi)$, whereas the second term contains all corrections.

Using (1), we rewrite the integral in the second term as

$$\begin{aligned}&\int[1+AP_n(\phi)\cos\zeta]e(\zeta,y)Q(y)d\zeta\,dy\\&=\int\left[1+A\frac{(\alpha+\mathbf{P}_\Sigma\cdot\mathbf{q})\mathbf{q}\cdot\mathbf{s}}{1+\alpha\mathbf{P}_\Sigma\cdot\mathbf{q}}\right]e(\zeta,y)Q(y)d\zeta\,dy\\&+\sin\phi\int A\left[\frac{\mathbf{P}_\Sigma\times\mathbf{q}\cdot\mathbf{s}}{1+\alpha\mathbf{P}_\Sigma\cdot\mathbf{q}}\right](1-\alpha^2)^{1/2}e(\zeta,y)Q(y)d\zeta\,dy\\&+\cos\phi\int A\left[\frac{\mathbf{P}_\Sigma\cdot\mathbf{s}-(\mathbf{P}_\Sigma\cdot\mathbf{q})(\mathbf{q}\cdot\mathbf{s})}{1+\alpha\mathbf{P}_\Sigma\cdot\mathbf{q}}\right]\\&\qquad\times(1-\alpha^2)^{1/2}e(\zeta,y)Q(y)d\zeta\,dy,\end{aligned}$$

where the integrals on the right-hand side of the equation are now independent of ϕ. If we denote these integrals by I_1, I_2, and I_3, the expression for $\ln\mathfrak{L}(\phi)$ becomes

$$\ln\mathfrak{L}(\phi)=\sum\ln[1+AP_n(\phi)\cos\zeta]-N\ln(I_1+I_2\sin\phi+I_3\cos\phi). \quad (8)$$

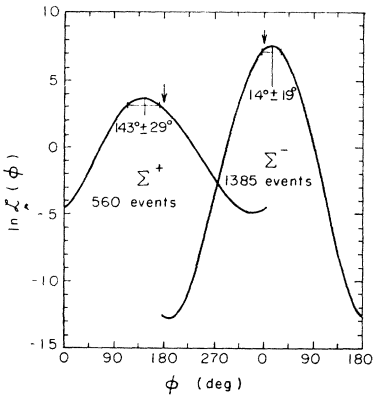

FIG. 6. $\ln\mathcal{L}(\phi)$ as a function of ϕ. The arrows at 180 and 0 deg indicate the expected values of ϕ assuming time-reversal invariance and neglecting final-state interactions.

Since an analytic expression for $Q(y)$ is unknown, I_1, I_2, and I_3 were calculated by using the 33 000 Monte Carlo events described above. The integrands of I_1, I_2, and I_3 depend on A, α, $\mathbf{P}_\Sigma$, $\mathbf{q}$, ζ, e, and Q. Of these A, α, $\mathbf{P}_\Sigma$, $\mathbf{q}$, and ζ are specified by each Monte Carlo event. For each event a numerical integration over ζ was performed by varying ζ between 0 and 2π. For each value of ζ the projected length and the dip of the recoil proton were calculated and e was obtained from the curves of Fig. 5. Since the Monte Carlo events are distributed as $Q(y)$, the integrals I_1, I_2, and I_3 are approximated by summing the numerical integrations over all events. These sums are normalized by dividing by the total number of Monte Carlo events.

The logarithms of the corrected likelihood functions,

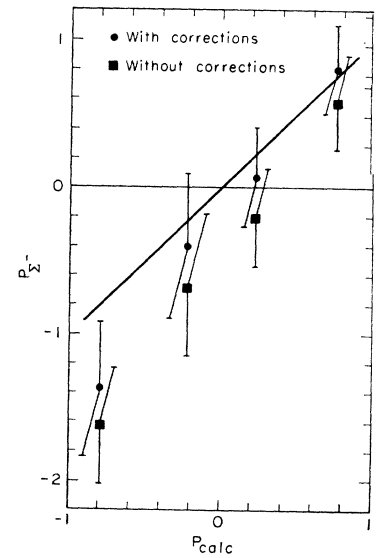

FIG. 7. Measured values of P_{Σ^-} as a function of the calculated value P_{calc}. The measured values should lie on a straight line with unit slope.

as given by (8), are shown in Fig. 6. From these likelihood functions, we obtain

$$\phi_-=14\pm19 \text{ deg}, \quad \phi_+=143\pm29 \text{ deg}.$$

These values are practically unchanged for any reasonable values of α_- and α_+.

For $\Sigma_+{}^+$, $\phi_+=180$ deg is 1.4×10^3 times as likely as $\phi_+=0$ deg, and for $\Sigma_-{}^-$, $\phi_-=0$ deg is 5.3×10^8 times as likely as $\phi_-=180$ deg.[12]

In view of the uncertainty in the detection efficiency e, one may question the entire correction procedure. However, ϕ is quite insensitive to the corrections that have been applied. The uncorrected values are

$$\phi_-=15\pm19 \text{ deg}, \quad \phi_+=148\pm28 \text{ deg}.$$

We were originally led to study the corrections because without them the following consistency check gave rather poor results.

Given ϕ (the sign of γ), it is possible to regard (7) as a function of P_Σ, thus giving an additional check on the Σ^- polarization. As before, the sample is broken up into four bins according to predicted polarization. We obtain P_Σ for each bin, again using the maximum-likelihood method. The appropriate correction integrals for each bin were evaluated by using the same method as used in the measurement of ϕ. Figure 7 exhibits the results with and without the corrections. Without the corrections the χ^2 confidence level is about 11%, while with corrections it is 67%. The corrections are only weakly dependent on the exact form of the detection efficiency functions. Despite the high confidence level for this consistency check, we cannot rule out the possibility of some residual bias in our data; however, because of the insensitivity of ϕ to the corrections that have been made, any residual bias should be negligible.

Our results are consistent with the $\Delta I=\frac{1}{2}$ rule, the theoretical predictions, and the previous measurements of ϕ. The statistical uncertainty is so large as to provide essentially no test of small violations of time-reversal invariance.

ACKNOWLEDGMENTS

We appreciate the diligent efforts of the 25-in. bubble chamber crew and the Bevatron staff. We gratefully acknowledge the indispensable help of our scanning and measuring personnel. We are particularly grateful for the cooperative assistance of our data librarian, Mrs. Natalie Groteguth. Finally, we thank Roger Gearhart for his help in designing, operating, and maintaining our beam.

[12] The values $\phi=0$ deg and $\phi=180$ deg are expected only if final-state interactions are neglected. If one takes into account final-state interactions one expects $\phi_+\approx166$ deg and $\phi_-\approx-1$ deg, in better agreement with our experimental values. A discussion of this is given by Roger O. Bangerter, Ph.D. thesis, University of California Radiation Laboratory Report No. UCRL-19244, 1969 (unpublished).